JOURNAL OF GEOPHYSICAL RESEARCH, VOL. 103, NO. D11, PAGES 13,169–13,180, JUNE 20, 1998

#60

Measurements of C_2–C_7 hydrocarbons during the Polar Sunrise Experiment 1994: Further evidence for halogen chemistry in the troposphere

P. A. Ariya,[1] B. T. Jobson,[2] R. Sander, H. Niki,[3] and G. W. Harris
Centre for Atmospheric Chemistry and Department of Chemistry, York University, North York, Ontario, Canada

J. F. Hopper and K. G. Anlauf
Atmospheric Environment Service, Downsview, Ontario, Canada

Abstract. Air samples for nonmethane hydrocarbon (NMHC) analysis were collected at two ground-based sites: Alert, Northwest Territories (82.5°N, 62.3°W) and Narwhal ice camp, an ice floe 140 km northwest of Alert, from Julian days 90 to 117, 1994, and on a 2-day aerial survey conducted on Julian days 89 and 90, 1994 over the Arctic archipelago. Several ozone depletion events and concurrent decreases in hydrocarbon concentrations relative to their background levels were observed at Alert and Narwhal ice camp. At Narwhal, a long period (≥7 days) of ozone depletion was observed during which a clear decay of alkane concentration occurred. A kinetic analysis led to a calculated Cl atom concentration of 4.5×10^3 cm^{-3} during this period. Several low-ozone periods concurrent with NMHC concentration decreases were observed over a widespread region of the Arctic region (82°–85°N, and 51°–65°W). Hydrocarbon measurements during the aerial survey indicated that the low concentrations of these species occurred only in the boundary layer. In all ozone depletion periods, concentration changes of alkanes and toluene were consistent with Cl atom reactions. The changes in ethyne concentration from its background level were in excess of those expected from Cl atom kinetics alone and are attributed to additional Br atom reactions. A box modeling exercise suggested that the Cl and particularly Br atom concentrations required to explain the hydrocarbon behavior are also sufficient to destroy ozone.

1. Introduction

The depletion of O_3 in the boundary layer at the onset of 24 hour daylight in the spring has been reported for several locations in the high Arctic such as Alert (82.5°N, Northwest Territories, Canada) [*Barrie et al.*, 1988; *Mickle et al.*, 1989; *Bottenheim et al.*, 1990; *Barrie et al.*, 1994; *Jobson et al.*, 1994]; Point Barrow (71°N, Alaska, United States) [*Oltmans et al.*, 1989] and Spitsbergen-Svalbard (74°–78°N, Norway) [*Solberg et al.*, 1994]. *Barrie et al.* [1988] first reported an anticorrelation between filterable bromine and ozone and between bromoform and ozone. This observation led them to suggest Br atom–initiated destruction of ozone. Clear decreases in the concentrations of C_2–C_4 alkanes were observed during the ozone depletion events which cannot be explained by Br chemistry [*Bottenheim et al.*, 1990; *Kieser et al.*, 1993] since Br reacts very slowly with most nonmethane hydrocarbons (NMHCs), especially alkanes [*Russell et al.*, 1988a]. *McConnell and Henderson* [1993] suggested that Cl atoms, which react much faster toward hydrocarbons, may be involved in the destruction of these molecules. However, it was not until the Polar Sunrise Experiment (PSE) 1992, that the first substantial evidence for the importance of Cl reactions was provided by *Jobson et al.* [1994] by using measurements of C_2–C_5 alkanes and matching their behavior during the ozone depletion events to that which would arise through Cl atom reactions. In the same campaign, observations of alkylnitrate concentration changes during ozone depletion were also consistent with Cl chemistry [*Muthuramu et al.*, 1994].

Hydrocarbons such as nonmethane alkanes, toluene, ethene, ethyne, and benzene are primarily emitted into the atmosphere through industrial activities and fossil fuel production and combustion [*Warneck*, 1988]. These hydrocarbons are transported from the source regions to more remote areas such as the Arctic. During transport, photochemical processes mainly initiated by HO radicals are involved in removing these nonmethane hydrocarbons at different rates. In addition to hydroxyl radicals, Cl atoms may play a significant role in the removal of some hydrocarbons in certain regions of the globe such as the marine boundary layer and the Arctic [*Pszenny et al.*, 1993; *Jobson et al.*, 1994]. Also, Br atoms may play an important role in the destruction of some unsaturated hydrocarbons in the troposphere [*Jobson et al.*, 1994]. The relative reaction rates for HO radical–initiated reactions with hydrocarbons are different from those for Cl or Br atom reactions. Hence the relative rates of removal of hydrocarbons can be used as an indicator for the dominance of particular atmospheric photochemical reactions such as those initiated by HO radicals or those started by Cl or Br atoms.

[1]Now at Air Chemistry Division, Max Planck Institute for Chemistry, Mainz, Germany.
[2]Now at NOAA Aeronomy Laboratory, Boulder, Colorado.
[3]Deceased April 1, 1995.

Paper number 98JD00284.
0148-0227/98/98JD-00284$09.00

Gas phase Cl atom and Br atom production and subsequent ozone destruction in various atmospheric processes have been considered [*Schroeder and Urone*, 1974; *Finlayson-Pitts*, 1983; *Barrie et al.*, 1988; *Finlayson-Pitts et al.*, 1989; *Keene et al.*, 1990; *McConnell et al.*, 1992; *Fan and Jacob*, 1992; *Pszenny et al.*, 1993; *Zetzsch and Behnke*, 1993; *Mozurkewich*, 1995]. The observation of BrO, the product of Br atom reaction with ozone during PSE 92, provided further evidence for the presence of reactive gas phase bromine [*Hausmann and Platt*, 1994]. The reactions of halides with O_3 have also been suggested, where ozone destruction occurs heterogeneously [*Hoigne et al.*, 1985; *Staehlin and Hoigne*, 1982]. Which of several possible mechanisms for the production of reactive halogen species is actually occurring in the Arctic is an open question which needs further research.

This paper reports measurements of C_2–C_7 hydrocarbons from two ground-based sites, Alert and Narwhal ice camp as well as from a 2-day aerial survey conducted on Julian days 89 and 90, 1994 (Julian day 1 = January 1) over the Arctic archipelago. This PSE was designed to further explore the phenomenon of ozone depletion and the observed coincident decrease in the concentration of alkanes. The samples were taken from Julian days 90 to 117, the period after the polar sunrise. By using a wide range of hydrocarbons as indicators of photochemical processes, and by sampling at several locations over the Arctic Ocean, this study has attempted to evaluate the extent of halogen chemistry in the Arctic troposphere.

2. Experiment

Grab sampling was conducted at the special studies laboratory at Alert from Julian days 90 to 117 for a total of 36 samples. Up to six samples were taken daily. Five of the samples were taken near buildings at Alert station. Grab sampling was conducted on Narwhal ice camp from Julian days 97 to 115 for a total of 97 samples. Thirteen samples were taken of interstitial air in the surface snowpack. The results of interestitial air samples are not presented here. Up to eight samples were taken daily at this location. Another 38 samples were taken on the Julian days 89 and 90 aerial survey, providing air samples from the surface layer and free troposphere covering a latitude range of approximately 82°–85°N, and 51°–65°W longitude.

The details of experimental procedures for hydrocarbon analysis are available elsewhere [*Jobson*, 1994]. Briefly, air samples were collected in 3.2 L SUMMA electropolished stainless steel canisters (Biospherics Research Corporation, Oregon) pressurized to 250 kPa by means of a Teflon diaphragm pump (KNF Neuberger, Incorporated). All connections, fittings, and sampling lines were stainless steel. The canisters were sent evacuated. At ground sites, canisters were filled and purged twice before taking samples. However, for aerial survey sampling, because of time limitation, samples were taken without prior flushing. Tests were carried out to investigate any potential difference between grab samples taken with and without prior flushing. No significant difference was observed. Replicate samples taken at Alert and Narwhal ice camp showed very good agreement ($\leq$5%).

Canisters were returned to York University in Toronto for analysis. C_2–C_8 hydrocarbons were measured using a gas chromatograph (GC) (Hewlett Packard 5890A) equipped with a flame ionization detector (FID) and a 50 m × 0.32 mm Al_2O_3/KCl PLOT column. About 1 L of the air sample was preconcentrated using a two-stage cryotrapping procedure. Air samples were passed through a 15 cm long Teflon tube cooled by dry ice to 223 K to remove moisture and a K_2CO_3 trap to remove CO_2 from the air samples. Previous tests indicated that C_2–C_7 hydrocarbons were not lost in the moisture trap. For C_8 hydrocarbons a loss of up to 10% was observed. In the first cryotrapping stage, hydrocarbons were condensed in a 0.3 cm diameter stainless steel loop packed with 60/80 mesh glass beads, and cooled with liquid argon. This loop was then heated, and the sample was flushed with helium to a second refocusing trap. This second trap, consisting of a 15 cm nickel capillary tube cooled with liquid nitrogen, was then flash heated to inject samples onto the column. The column was temperature programmed from 313 to 343 K at 5 K min^{-1}, then ramped at 25 K min^{-1} to 403 K, followed by 7 K min^{-1} to 473 K, with isothermal operation at 473 K for 15 min. Helium was used as the carrier gas, operated at a head pressure of 250 kPa. Air samples were analyzed within a month and a half of collection.

Canisters were cleaned by evacuation to an ultimate pressure of 3×10^{-4} Pa while heating at 358 K in an oven for at least 2.5 hours. To check for system contamination, blanks, consisting of a canister filled with ultrahigh purity helium, were run periodically. Blank samples were clean with respect to the lowest concentration of hydrocarbons of interest. Previous tests indicated that traveling blanks, consisting of cleaned, evacuated canisters sent to Alert and returned empty to York University, were clean except for the presence of up 20 parts per trillion by volume (pptv) of several alkenes, including ethene and propene. The generation of alkenes in sample canisters has been observed by our group previously and appears to be related to canister sampling history, being more noticeable for canisters that have been used in urban air sampling.

Identification and quantification of NMHC species were made using reference gas mixtures blends (Conservation and Protection Service, Environment Canada). The standard mixtures, containing about 5 ppbv of C_2–C_8 alkanes, alkenes, and alkynes were loaded onto the GC system exactly the same way as the air samples. The quantitation limit based on FID response and baseline noise was approximately 5 pptv for the C_5 hydrocarbons in a 1 L sample. Most species (C_2–C_5 alkanes) were at mixing ratios well above the quantitation limit for a major part of the sampling period and therefore the precision was of the order of 1%. Note that our laboratory participated in few rounds of International Hydrocarbon Intercomparison Experiments since November 1991. Results for most species were within about 10% of those of the National Institute for Standards and Technology (NIST) and the National Center for Atmospheric Research (NCAR).

Ozone was measured continuously at the Alert background chemistry laboratory using a Teco model 49 analyzer. The detection limit is estimated at 0.5 ppbv, and the accuracy of the hourly averages was within 2%.

3. General Characteristics of the Measurement Periods

3.1. Narwhal Ice Camp

A detailed description of the site, along with chemical and meteorological measurements made at Narwhal ice camp are given elsewhere [*Hopper et al.*, 1998]. The maximum ozone

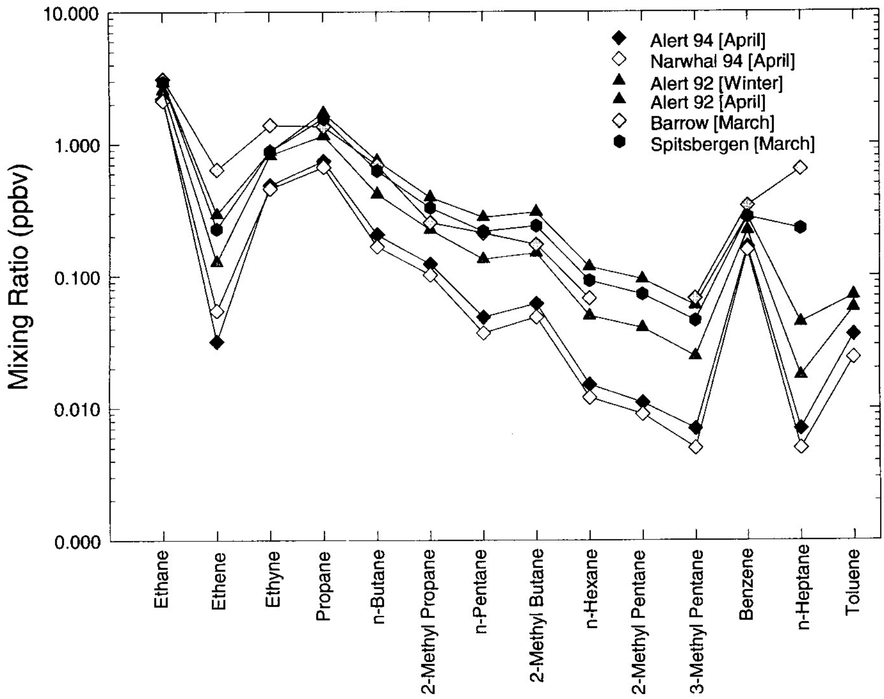

Figure 1. Comparison of average C_2–C_7 hydrocarbon concentrations at Alert and Narwhal ice camp during April 1994 with winter/spring values at Alert in 1992 and other remote northern hemisphere sites. Concentrations are plotted on a log scale.

mixing ratio observed at the Narwhal ice camp was about 36 ppbv. A long period of ozone depletion (≥7 days) was observed at the beginning of the grab sampling period (section 5.1, Figures 2a and 2b). The 5-day back trajectories of air parcels reaching the Narwhal ice camp at the 1000 hPa level were calculated. The position of the air parcels 5 days earlier was used to assign a representative source region for the air. For the ozone-depleted period from Julian day 94 to 99, back trajectories indicated that the air had its origin over the Arctic Ocean. From Julian days 99 to 109 a very stagnant air parcel was present at Narwhal. The air had originated from some point on the Arctic Ocean in proximity to the Hazen Plateau and traveled only over the coastal area around the Hazen Plateau and the Baffin Bay. On Julian days 110 to 112, air reaching Narwhal had been transported long distances from the southeast and had traveled at least 3 days along the coastal regions of Greenland. On Julian days 113 to 116 the air parcels had originated from the Arctic Ocean and had spent the previous 5 days there. The surface air temperature was on average about 238 K from Julian days 94 to 108, and then increased to approximately 258 K around Julian day 111 and decreased to approximately 248 K for the rest of the sampling period.

3.2. Alert

The detailed meteorology at Alert during this campaign is given by *Hopper et al.* [1998]. During PSE 94, several minor ozone depletion events were observed in April. Five-day back trajectories for air parcels during the ozone depletions observed from Julian days 95 to 98 indicated that the air originated over the Arctic Ocean. The interpretation of trajectories for minor depletion events later in April is more complicated. As pointed out by *Hopper et al.* [1998], these events are more likely representative of a nonsteady state situation. In addition, on some occasions the complex topography of this region may contribute to errors in the calculation of trajectories. *Hopper et al.* [1994] and *Worthy et al.* [1994] discussed that the interpretation of trajectories and concentrations at this site can be done most reliably when there is a strong and persistent synoptic flow such as that observed during Julian days 95 to 98. The air temperature was on average about 238 K from Julian days 94 to 108, and then increased to about 263 K around Julian day 111 and decreased to approximately 252 K for the rest of the sampling period.

4. Distribution of Hydrocarbon Species

The average concentrations and relative distribution of C_2–C_7 hydrocarbons are compared to those measured previously at high-latitude northern hemisphere sites in Figure 1. In Figure 1, average concentrations at Narwhal ice camp and Alert, during periods of "normal" ozone concentrations (O_3 mixing ratio ≥30 ppbv) during April 1994 are compared to measurements made at Alert during winter (January and February) and spring (April) [*Jobson et al.*, 1994], as well as with those taken during the month of March in Spittsbergen [*Hov et al.*, 1984] and Barrow [*Doskey and Gaffney*, 1992]. As seen in Figure 1, the average concentrations of alkanes (≥C_3) observed at Narwhal ice camp and Alert (1994) during the month of April (excluding ozone depletion episodes) are markedly lower than other measurements. An exception is benzene, which shows little variability (less than a factor of 2) among all sites. Note that after polar sunrise in April the alkanes displayed a systematic decrease in concentration, with the larger alkanes displaying the largest concentration change. This behavior was observed in PSE 1992 and 1994 and is attributed to the increase in photochemistry associated with sunrise. Thus

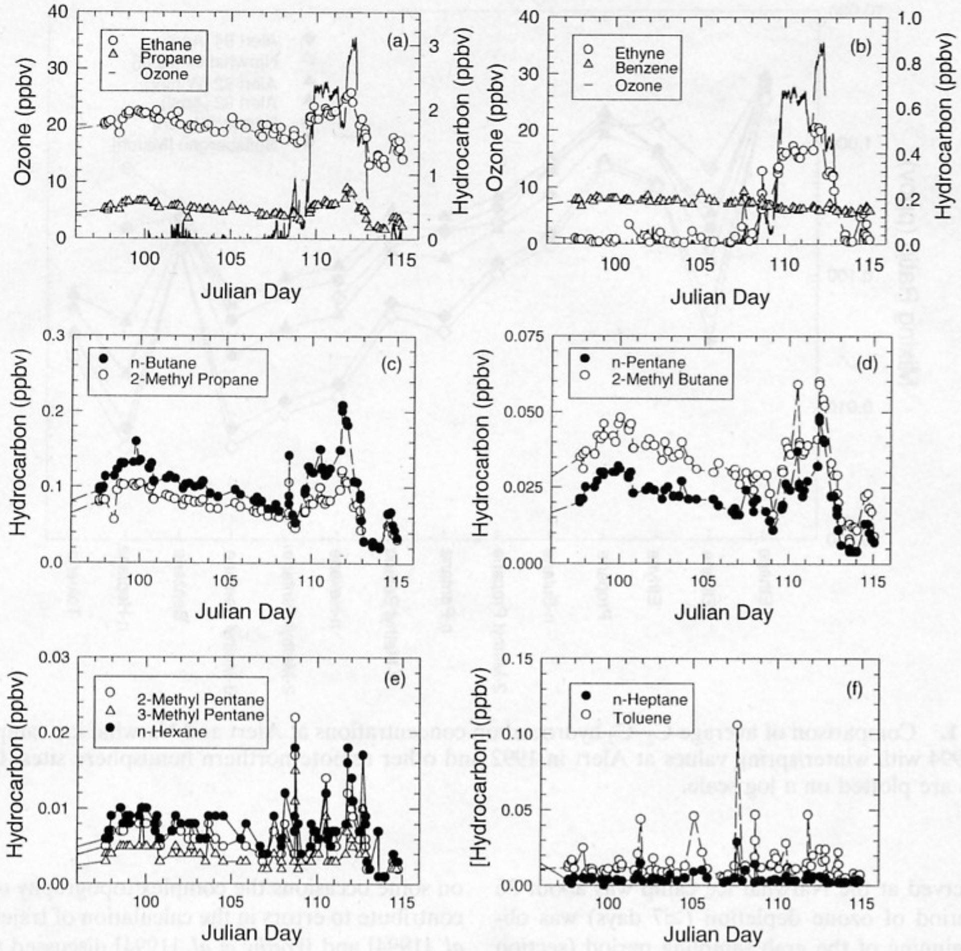

Figure 2. Time series for some C_2–C_7 hydrocarbons at Narwhal ice camp: (a) ethane, propane, and ozone (solid line); (b) ethyne, benzene, and ozone (solid line); (c) *n*-butane and 2-methyl propane; (d) *n*-pentane and 2-methyl butane; (e) *n*-hexane, 2-methyl pentane, and 3-methyl pentane; (f) *n*-heptane and toluene.

the average ethane concentration displays the smallest spatial variability (≤ factor of 1.3) for these springtime data sets, while average *n*-hexane concentrations displayed over a factor of 10 range. This indicates that measurements in which there were relatively lower concentrations of more reactive species correspond to more photochemically processed air mass. From the concentrations and distributions observed at these locations, we conclude that the Arctic air mass during winter and early spring is fairly homogeneous for NMHC species with long lifetimes such as C_2–C_7 alkanes, toluene, ethyne, and benzene. Sources of these hydrocarbons appear to be similar and suggest fossil fuel combustion and production.

5. Time Series Profiles

5.1. Narwhal Ice Camp

Time series for concentrations of the major C_2–C_7 NMHCs are shown in Figure 2. Alkanes, toluene, and ethyne correlate well with each other. The correlation coefficients (r^2) among most NMHCs are greater than 0.8 with the exception of benzene, which displayed the smallest concentration variability and did not correlate well with other hydrocarbons. As depicted in Figures 2a and 2b, high concentrations of these species occurred when the ozone mixing ratios are high (≥30 ppbv). Low concentrations of these compounds were seen to occur when ozone concentration fell to zero or near-zero values. The benzene concentration did not change drastically during ozone depletion episodes; rather, it displayed a gradual decline from the beginning to the end of the sampling period. The concentration of higher alkanes (≥C_6) approaches the detection limit, especially during ozone depletion events. Ethene concentrations showed very large variability and are not considered reliable, especially since the range of variability is comparable to the magnitude of the artifact observed in the traveling blank canisters.

5.2. Alert

There are more rapid fluctuations in the observed NMHCs at Alert than at Narwhal ice camp. Examples of time series for the concentrations of the major C_2–C_7 alkanes, toluene, ethyne, and benzene are shown in Figures 3a–3f. The correlation coefficients (r^2) among most NMHCs were greater than 0.8; again the exception is benzene. Shown in Figures 3a and 3b are plots of time series of some selected hydrocarbons and ozone. All alkanes, toluene, and ethyne show a positive correlation with ozone. Benzene concentration did not show a marked decline or recovery during low- and high-ozone episodes. However, as at Narwhal, benzene concentrations showed a slow decline from the beginning to the end of the sampling period. Depicted in Figure 4a is the plot of methane

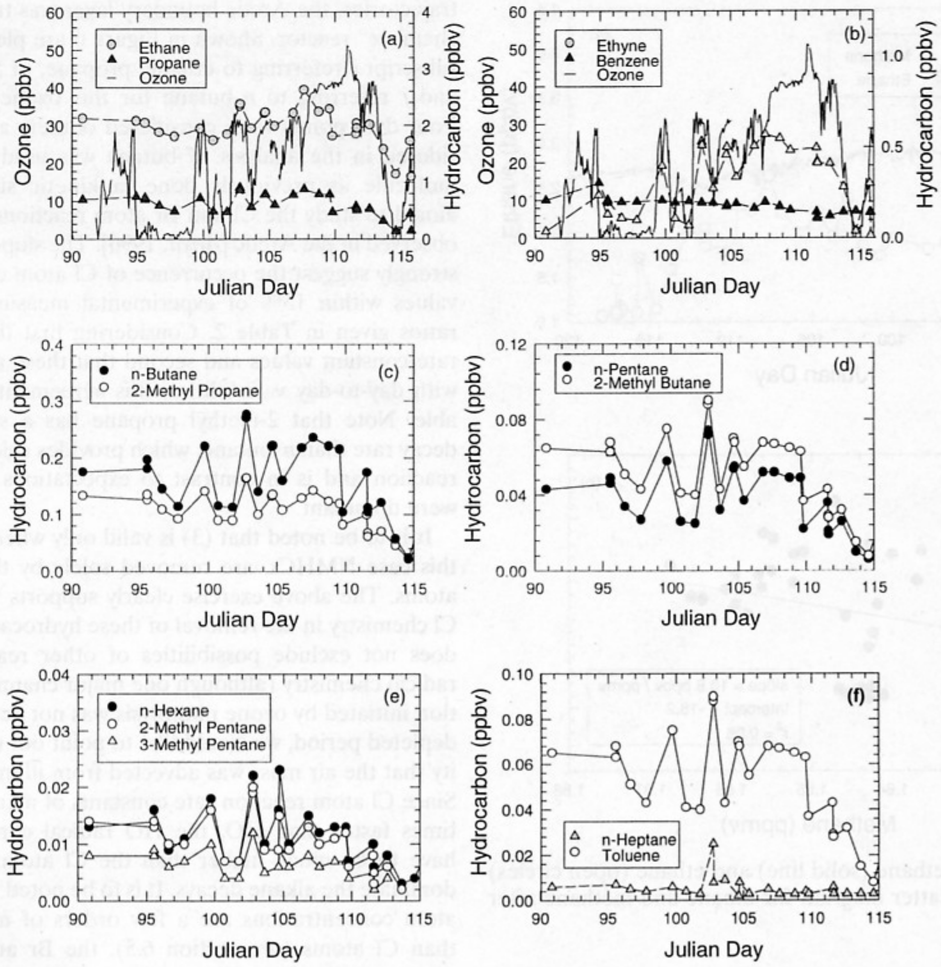

Figure 3. Time series for some C_2–C_7 hydrocarbons at Alert: (a) ethane, propane, and ozone (solid line); (b) ethyne, benzene, and ozone (solid line); (c) *n*-butane, and 2-methyl propane; (d) *n*-pentane and 2-methyl butane; (e) *n*-hexane, 2-methyl pentane, and 3-methyl pentane; (f) *n*-heptane and toluene.

and ethane concentration at Alert. Figure 4b shows the correlation between methane and ethane at the same location. In contrast to the dark period, where methane and ethane correlated very well [*Jobson et al.*, 1994], in the light period, the subject of this study, this correlation is much poorer.

5.3. Airborne Measurements

Of a total of 38 samples, 24 were taken in the boundary layer at altitudes of 170–680 m and 14 in the free troposphere at altitudes between 680 and 1700 m. Shown in Figures 5a–5f are examples of plots of hydrocarbon concentrations versus the altitude for samples taken in the aerial survey. Most alkanes correlated well with one another as well as with toluene and ethyne. Of the alkanes, ethane showed the least correlation with the other NMHCs. Benzene concentrations between boundary layer samples and free tropospheric samples were indistinguishable within the measurement uncertainties. As shown in Figures 5a–5f, low ozone mixing ratios (≤10 ppbv) were observed at altitudes below 700 m. High hydrocarbon concentrations were observed when ozone mixing ratios were at normal levels (≥30 ppbv).

6. Hydrocarbon and Ozone Concentration Changes and Halogen Chemistry

6.1. Isomeric Ratios and Distinction Between HO and Cl Chemistry

Shown in Table 1 are Cl, HO, and Br rate constants at 243 K for ozone and a series of NMHCs measured during this study. Some general features of the hydrocarbon kinetics can be used to distinguish between Cl atom and HO radical chemistry. For instance, the Cl atom rate constant of an alkane is generally about 2 orders of magnitude faster than for HO radicals [*Ariya Hooshiyar and Niki*, 1995; *Atkinson et al.*, 1992]. Also, HO radical rate constants for normal alkanes and isoalkanes are very similar; however, isoalkanes have significantly lower Cl atom rate constants than the corresponding *n*-alkanes (e.g., the Cl atom rate constant for 2-methyl propane is about 0.67 that of *n*-butane [*Ariya Hooshiyar and Niki*, 1995]).

In contrast to alkanes, benzene reacts more slowly with Cl atoms than HO radicals [*Ariya et al.*, 1998]. Thus if Cl chemistry is dominant, the change in the concentration of benzene is negligible. Hence benzene can be used as a zero point for the Cl atom kinetic analysis of NMHCs. The temperature depen-

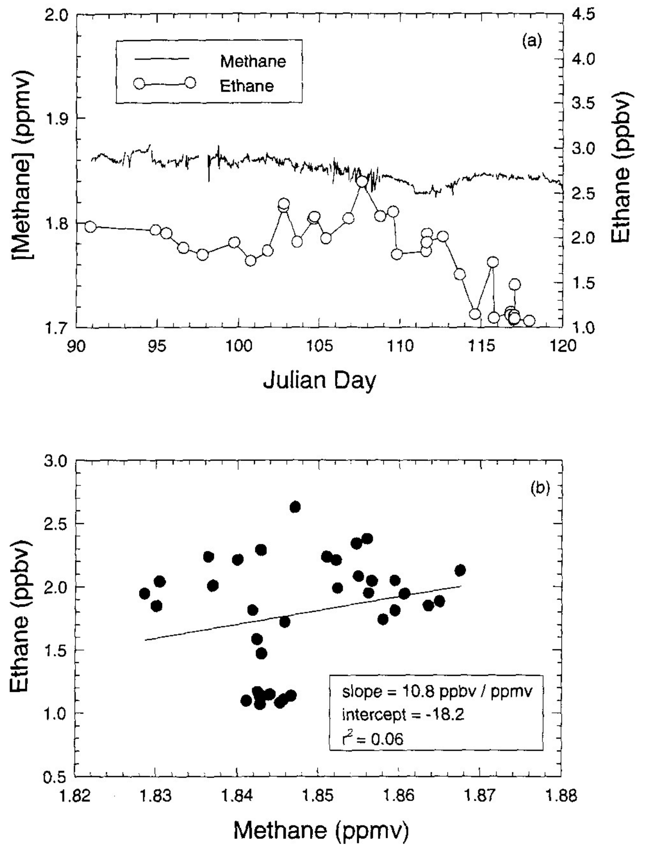

Figure 4. (a) Methane (solid line) and ethane (open circles) time series. (b) Scatter diagram for ethane and methane after polar sunrise.

dency for the Cl plus alkane rate constants is small. For example, the Cl plus ethane rate constant at 243 K is only 15% lower than at 296 K [*Atkinson et al.*, 1992]. For the Cl atom rate constant of benzene and toluene, the preliminary low-temperature GC results of recent work by *Ariya* [1996] indicated that toluene does not have a significant temperature dependence, and the very conservative upper limit of Cl atom reaction rate constant for benzene of 1×10^{-12} cm^3 molecule^{-1} s^{-1} was obtained at 243 K.

6.2. Cl Atom Signature in the Absence of Ozone

Depicted in Figure 2, alkanes show a slight decrease in their concentration from Julian days ~99 to 108 in Narwhal ice camp (PSE 94). During this period, no measurable ozone was observed. The detection limit for the ozone monitor was 0.5 ppbv. If Cl atoms are indeed the only oxidants involved in the removal of alkanes, then the following reactions will occur:

$$\mathrm{Cl\cdot} + \mathrm{RH}_i \rightarrow \mathrm{R}_i + \mathrm{HCl} \quad (1)$$

$$\mathrm{Cl\cdot} + \mathrm{RH}_j \rightarrow \mathrm{R}_j + \mathrm{HCl} \quad (2)$$

where RH_i and RH_j denote the ith and jth alkanes. Thus the integrated relative rate equation can be written as

$$\ln \{[\mathrm{RH}_i]_{t1}/[\mathrm{RH}_i]_{t2}\} = (k_i/k_j) \ln \{[\mathrm{RH}_j]_{t1}/[\mathrm{RH}_j]_{t2}\} \quad (3)$$

According to (3), plots of $\ln \{[\mathrm{RH}_i]_{t1}/[\mathrm{RH}_i]_{t2}\}$ versus $\ln \{[\mathrm{RH}_j]_{t1}/[\mathrm{RH}_j]_{t2}\}$ should yield straight lines with the slope equal to k_i/k_j and zero intercept. Since the Arctic air mass was very stagnant during this period, as indicated by 5-day back trajectories, the Arctic boundary layer was treated as a "smog chamber" reactor. Shown in Figure 6 are plots of (3) with the subscript i referring to ethane, propane, or 2-methyl propane and j referring to n-butane for this ozone-depleted period. Four data points were considered outliers and were not considered in the analysis. N-butane was used as the reference molecule as previously done in kinetic studies specifically aimed to study the Cl and Br atom reactions of hydrocarbons observed in the Arctic [*Ariya*, 1996]. The slopes ($k_{\mathrm{RH}}/k_{n\text{-butane}}$) strongly suggest the occurrence of Cl atom chemistry, with all values within 15% of experimental measured rate constant ratios given in Table 2. Considering first the uncertainty on rate constant values and second that these are real field data with day-to-day variabilities, this agreement is quite remarkable. Note that 2-methyl propane has a significantly lower decay rate than n-butane, which provides evidence for Cl atom reaction and is in contrast to expectations if HO chemistry were dominant.

It is to be noted that (3) is valid only when the reactants, in this case NMHCs, are removed solely by the reaction of Cl atoms. The above exercise clearly supports the dominance of Cl chemistry in the removal of these hydrocarbons; however, it does not exclude possibilities of other reactions, even HO radical chemistry (although one major channel of HO production initiated by ozone photolysis was not active in this ozone-depleted period, we would like to point out the slight possibility that the air mass was advected from illuminated latitudes). Since Cl atom reaction rate constants of alkanes are up to 100 times faster than HO, the HO radical concentration would have to be much higher than the Cl atom concentration to dominate the alkane decays. It is to be noted that even if the Br atom concentrations are a few orders of magnitudes higher than Cl atoms (see section 6.5), the Br atom reaction rate constants are still much too slow to account for the observed concentration changes of the alkanes.

6.3. Calculation of [Cl]

During this period, from Julian days 99 to 108 at Narwhal, we make the assumption that the hydrocarbon trends are a result of oxidative removal by reaction with Cl atoms and neglect for the moment changes in concentration that may occur as a result of mixing processes. Equation (4) was used to calculate the Cl atom concentration from the hydrocarbon trends over reaction time t, using only those species which could be quantified reliably:

$$[\text{molecule}]_{t1} = [\text{molecule}]_{t2} \exp \int (-k_{\mathrm{Cl}}[\mathrm{Cl}]\, dt) \quad (4)$$

where the product of k_{Cl}, the Cl atom rate constant, and [Cl], the Cl atom concentration, is integrated over the reaction time t. The rate coefficients of the examined NMHCs with Cl atoms are relatively temperature insensitive. Thus under a strictly chemical kinetic environment, for molecules such as hydrocarbons, a plot of ln ([hydrocarbon]$_{t1}$/[hydrocarbon]$_{t2}$) versus k_{Cl} should be linear with slope equal to the term $-\int [\mathrm{Cl}]\, dt$.

In Figure 7 the hydrocarbon concentration changes at Narwhal for period of Julian days 100–108 are plotted against Cl atom rate coefficients at the average ambient temperature of 248 K. An average concentration from four samples at the beginning and end of the period was used to calculate [hydrocarbon]$_{t1}$ and [hydrocarbon]$_{t2}$, respectively. A linear regression through the C_2–C_4 alkane data yields a slope of -3.0

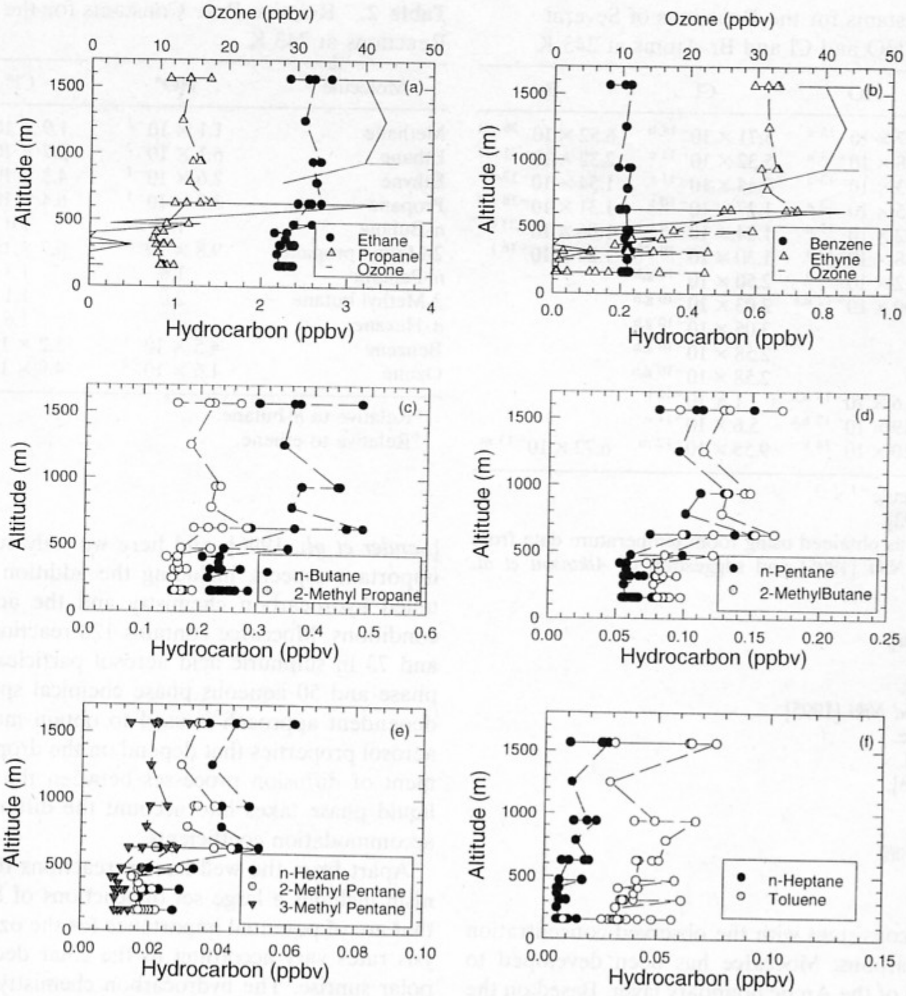

Figure 5. Vertical profiles for some C_2–C_7 hydrocarbons during the aerial survey: (a) ethane, propane, and ozone (solid line); (b) ethyne, benzene, and ozone (solid line); (c) *n*-butane and 2-methyl propane; (d) *n*-pentane and 2-methyl butane; (e) *n*-hexane, 2-methyl pentane, and 3-methyl pentane; (f) *n*-heptane and toluene.

($\pm$0.5; 2 s) $\times$ 10^9 atom cm^{-3} s. The mixing ratios of higher alkanes were close to or within our detection limit during this period and therefore not included in the regression. Dividing the slope by the 7.79-day period (Julian days 107.62 − 99.83; Δt = 7.79 days) spanned by the data yields an average Cl atom concentration of 4.5 ($\pm$0.7) $\times$ 10^3 cm^{-3}. Calculating Cl atom concentrations from different time intervals within the day 100–108 period yields a relatively small range of values. In the worse case a 40% deviation from the above value was obtained. The effect of mixing between ozone-depleted air and the free troposphere above will significantly increase the concentrations of most species with the exception of benzene, which reacts slowly with Cl and Br atoms and does not display a strong vertical gradient. Horizontal mixing must also be considered, but little is known about the horizontal extent of the phenomena. An observable effect of mixing on hydrocarbon trends can only manifest itself if significantly different mixing ratios of hydrocarbons have been blended together, that is, if the air masses being mixed have been chemically processed for different lengths of time. For instance, *Solberg et al.* [1996] have illustrated how mixing will influence hydrocarbon decay trends by assuming a single characteristic mixing time of 1 day for all hydrocarbons. Their study serves to show how air mass mixing will influence the short-lived species more than the long-lived species and thus lead to changes in the relative concentrations of the reactive alkanes. A strictly chemical model of the hydrocarbon trends will yield a lower limit on the actual radical concentrations. For the episode at Narwhal, conditions were very stagnant [*Hopper et al.*, 1998], and it is reasonable to assume that mixing effects were minimized. However, the halogen atom concentrations determined from the linear fit to the observed trends must be considered a lower limit.

Note that the lack of ozone during this period and the evidence of Cl atoms in the troposphere rules out the release of Cl atoms as the result of the reaction of Cl^- with O_3. In addition, the lack of ozone during this period at Narwhal indicates that a major source of NO_3 is absent. Consequently N_2O_5 formation during this period is likely to be insignificant. Hence a Cl atom source via suggested reactions between N_2O_5 and Cl^- seems to be unimportant under these conditions.

6.4. Modeling of Ozone-Depleted Period at Narwhal

In addition to the data evaluation explained above, we used a box model "MoccaIce" (model of chemistry considering aerosols in cold environments) to investigate what levels of

Table 1. Rate Constants for the Reactions of Several Hydrocarbons With HO and Cl and Br Atoms at 243 K

Molecule	HO	Cl	Br
Methane	2.07×10^{-15} [a]	3.71×10^{-14} [b]	6.52×10^{-26} [c,d]
Ethane	1.18×10^{-13} [a]	5.32×10^{-11} [e]	2.32×10^{-21} [c,d]
Ethyne	4.93×10^{-13} [a]	8.44×10^{-11} [e]	1.54×10^{-13} [f]
Propane	7.45×10^{-13} [a]	1.27×10^{-10} [g]	1.31×10^{-18} [c,d]
n-Butane	1.92×10^{-12} [a]	1.94×10^{-10} [g,h]	1.86×10^{-23} [c,i]
2-Methyl propane	1.88×10^{-12} [a]	1.30×10^{-10} [g,h]	1.24×10^{-16} [j]
n-Pentane	3.12×10^{-12} [a]	2.50×10^{-10} [g,h]	
2-Methyl butane	3.90×10^{-12} [h,k]	2.03×10^{-10} [g,h]	
n-Hexane		3.05×10^{-10} [g,h]	
2-Methyl pentane		2.58×10^{-10} [g,h]	
3-Methyl pentane		2.58×10^{-10} [g,h]	
Benzene	8.6×10^{-13} [h,k]	1×10^{-12} [l]	
Toluene	6.19×10^{-12} [h,k]	5.6×10^{-11} [e]	
Ozone	3.10×10^{-14} [k]	9.55×10^{-12} [m]	6.72×10^{-13} [m]

Units are cm^3 $molecule^{-1}$ s^{-1}.
[a]*Atkinson et al.* [1992].
[b]The 243 K value was obtained using room temperature data from *Ariya Hooshiyar and Niki* [1995] and suggestion of *Atkinson et al.* [1992].
[c]Estimated.
[d]*Russell et al.* [1988a].
[e]*Ariya* [1996].
[f]*Barnes et al.* [1993].
[g]*Ariya Hooshiyar and Niki* [1995].
[h]Room temperature.
[i]*Galiba et al.* [1964].
[j]*Russell et al.* [1988b].
[k]*Atkinson* [1986].
[l]*Ariya et al.* [1998a].
[m]*Nicovich et al.* [1990].

photooxidants are consistent with the observed concentration changes of hydrocarbons. MoccaIce has been developed to study the chemistry of the Arctic boundary layer. Based on the MOCCA model which was used to study marine air at midlatitudes [*Sander and Crutzen*, 1996], the model has now been modified to describe the polar sunrise in the Arctic. A more detailed description of MoccaIce has been given elsewhere [*Sander et al.*, 1996], and here we only summarize the most important aspects, including the addition of moderately detailed hydrocarbon chemistry and the adaptation to Arctic conditions. MoccaIce contains 120 reactions in the gas phase and 73 in sulphuric acid aerosol particles. There are 65 gas phase and 50 aqueous phase chemical species. A quasi-size-dependent approach is used to obtain mean values of those aerosol properties that depend on the droplet radii. The treatment of diffusion processes between the gas phase and the liquid phase takes into account the different solubilities and accommodation coefficients.

Table 2. Relative Rate Constants for the HO, Cl, and Br Reactions at 243 K

Molecule	HO[a]	Cl[a]	Br[b]
Methane	1.1×10^{-3}	1.9×10^{-4}	6.0×10^{-14}
Ethane	6.1×10^{-2}	2.7×10^{-1}	2.1×10^{-9}
Ethyne	2.6×10^{-1}	4.3×10^{-1}	1.4×10^{-1}
Propane	3.9×10^{-1}	6.4×10^{-1}	1.2×10^{-6}
n-Butane	1.0	1.0	1.7×10^{-11}
2-Methyl propane	9.8×10^{-1}	6.7×10^{-1}	1.1×10^{-4}
n-Pentane	1.6	1.3	
2-Methyl butane	2.0	1.1	
n-Hexane		1.6	
Benzene	4.5×10^{-1}	5.2×10^{-3}	
Ozone	1.6×10^{-2}	4.9×10^{-2}	6.2×10^{-1}

[a]Relative to *n*-butane.
[b]Relative to ethene.

Apart from the well-known reactions the chemical mechanism includes a large set of reactions of halogen compounds that are of potential importance for the ozone budget. Photolysis rates vary according to the solar declination during the polar sunrise. The hydrocarbon chemistry includes C_1–C_5 alkanes, ethene, ethyne, benzene, as well as the halocarbons CH_3Br and $CHBr_3$. Their initial reactions with HO radicals and Cl and Br atoms are considered. Secondary reactions of the intermediates have been simplified in the model by com-

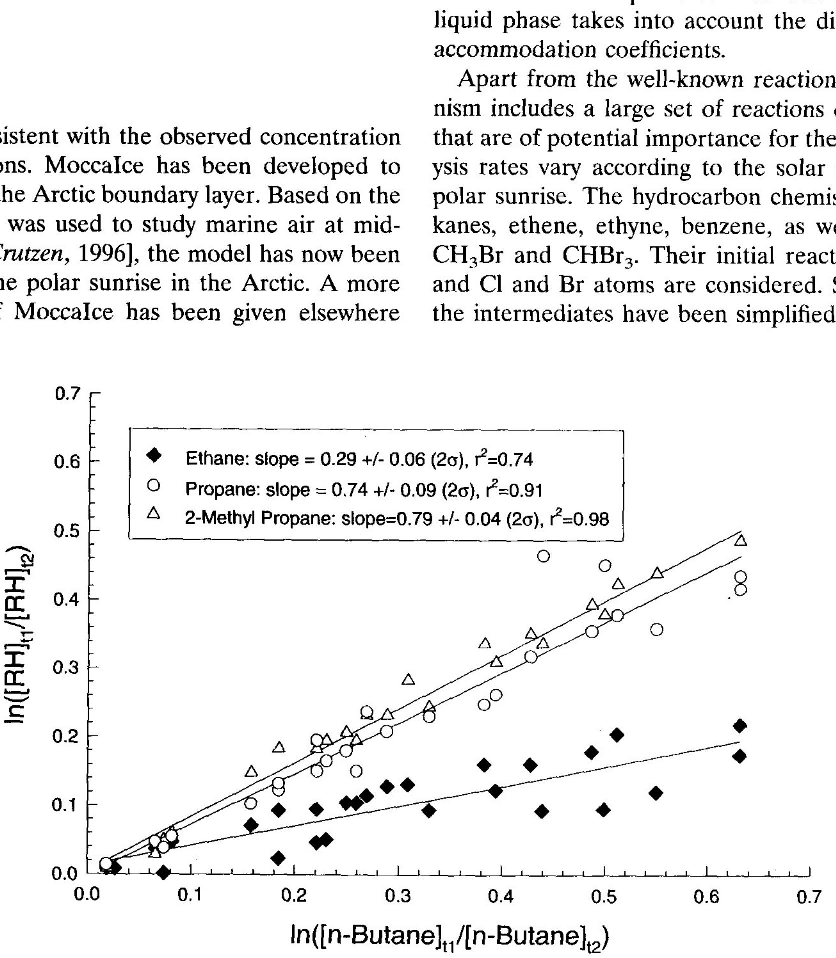

Figure 6. A plot of ln $([RH]_{t1}/[RH]_{t2})$ versus ln $([n\text{-butane}]_{t1}/[n\text{-butane}]_{t2})$ for the Julian days 99 to 108 period at Narwhal ice camp. The solid lines are least squares fits to the data, with corresponding slopes and correlation coefficients.

bining different alkyl groups into a generic R (e.g., RO, RO_2). The initial mixing ratios of hydrocarbons were set to the experimentally observed values at the beginning of the low-ozone period at Julian day 99. By using a Cl_2 flux into the system to maintain Cl atom concentrations of about 4×10^3 cm^{-3}, the observed hydrocarbon decay rate could be reproduced. In addition, a small bromine flux into the system was necessary to keep the modeled mixing ratio of O_3 below 0.5 ppbv, since a small amount of ozone was produced by NO_2 photolysis which was initially present at 20 pptv.

The chlorine flux was adjusted to match the observed hydrocarbon decay; thus the model does not reveal any more about the concentration of chlorine atoms than a simple kinetic expression, such as those used earlier. However, the model can be used to analyze the complex interaction between HO and Cl chemistry. The major HO production pathway under normal conditions is photolysis of O_3 to $O(^1D)$ followed by reaction with H_2O. In the ozone-depleted air mass, this channel obviously stops. Several other reactions now gain relative importance in HO production with photolysis of HNO_2 and HOBr now contributing significantly to the production of HO. Under the conditions of our model run, the reaction of ROOH with Cl is not an important HO source even if a yield of 100% for HO formation is assumed. HO_2 is quickly reduced to HO by reaction with NO; thus reactions that produce HO_2 can also be considered an indirect source of HO. HO_2 is produced in secondary steps of the oxidation of hydrocarbons:

$$RCH_2O + O_2 \rightarrow RCHO + HO_2 \quad (5)$$

Hence the oxidation of hydrocarbons also contributes to HO formation. In the model the reactions of alkanes with Cl and aldehydes with Br produce significant amounts of HO. Adding all HO formation pathways mentioned above, MoccaIce calculates noontime HO concentrations of about 10^5 cm^{-3} during the low-ozone period. The impact of HO reactions with light alkanes is found to be less important than corresponding Cl atom reactions at conditions described above. Benzene concentrations may show a decrease due to HO removal at the Narwhal ice camp, but this small change (of order of 3% assuming 4 days reaction time and HO = 10^5 cm^{-3}) cannot be reliably quantified due to the variability in the data, and so a meaningful comparison to model results could not be made.

Table 3. First-Order Regression Data From Plots of ln ($[molecule]_{low}/[molecule]_{bkg}$) Versus k_{Cl} for Ozone Depletion Episodes at Narwhal Ice Camp, Alert, and Airborne Measurements

Episode	Slope: $-\int [Cl]\, dt$, atoms cm^{-3} s	Correlation Coefficient (r^2)	y Intercept
Narwhal (Julian day 113)	$-8.1 (\pm 0.4) \times 10^9$	0.97	-0.16 ± 0.12
Alert (Julian day 114)	$-9.4 (\pm 0.5) \times 10^9$	0.93	-0.04 ± 0.08
Flight (pair 1)	$-3.1 (\pm 0.7) \times 10^9$	0.91	-0.02 ± 0.02
Flight (pair 2)	$-3.6 (\pm 0.4) \times 10^9$	0.99	-0.09 ± 0.07
Flight (pair 3)	$-3.8 (\pm 0.7) \times 10^9$	0.96	-0.01 ± 0.12
Flight (pair 4)	$-2.1 (\pm 0.2) \times 10^9$	0.97	0.01 ± 0.06

Stated uncertainties are 2 standard deviations.

6.5. Major Ozone Depletion Events

Various ozone depletion events were observed both at Alert and Narwhal ice camp. Back trajectories of these events indicated that the depleted air was transported from the Arctic Ocean (or ice-covered areas in close proximity to the ocean). We can assume "background" concentrations for NMHCs when the ozone mixing ratio is at its normal levels (≥30 ppbv). The change in concentration of a molecule from its "background" $[molecule]_{bkg}$ level to the concentration observed in ozone-depleted air, $[molecule]_{low}$, can be related to Cl atom reaction kinetics by (4). A plot of ln ($[molecule]_{low}/[molecule]_{bkg}$) versus k_{Cl} should be linear with slope equal to the term $-\int [Cl]\, dt$. Table 3 shows the value of the Cl atom action integral calculated from a series of ozone depletion events at the ground sites and those encountered during the aerial survey.

Figures 8 and 9 are plots showing these major events at Narwhal ice camp and Alert. Similarly, the flight data were evaluated by using high-altitude measurements as "back-

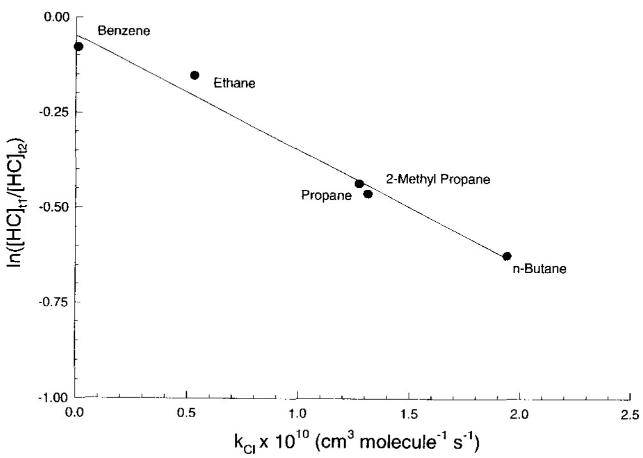

Figure 7. Correlation between logs of hydrocarbon concentration ratios in ozone-depleted air from normal ozone days against Cl atom rate constants for the Julian day 99–108 period at Narwhal ice camp. A least squares fit line has been drawn through the alkane and benzene data.

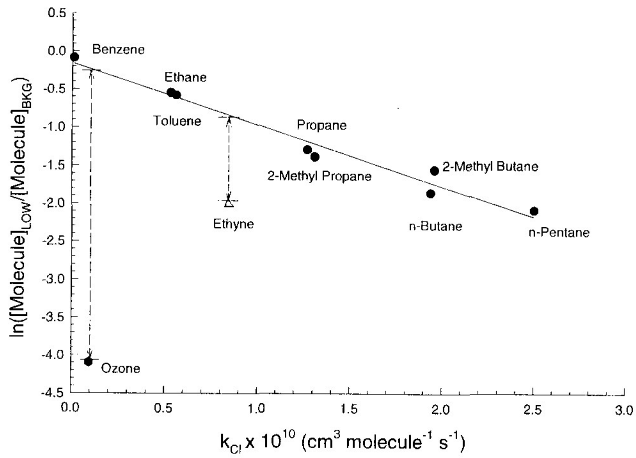

Figure 8. Correlation between logs of hydrocarbon concentration ratios in ozone-depleted air from normal ozone days against Cl atom rate constants for the Julian day 113 at Narwhal ice camp. A least squares fit line has been drawn through the alkane and benzene data. The deviations of ethyne and ozone from the expected Cl atom kinetics are represented by dashed lines.

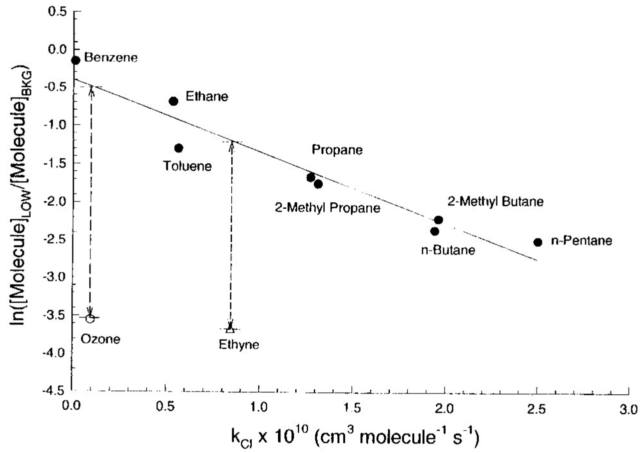

Figure 9. Correlation between logs of hydrocarbon concentration ratios in ozone-depleted air from normal ozone days against Cl atom rate constants for the Julian day 114, 1994 at Alert. A least squares fit line has been drawn through the alkane and benzene data. The deviations of ethyne and ozone from the expected Cl atom kinetics are represented by dashed lines.

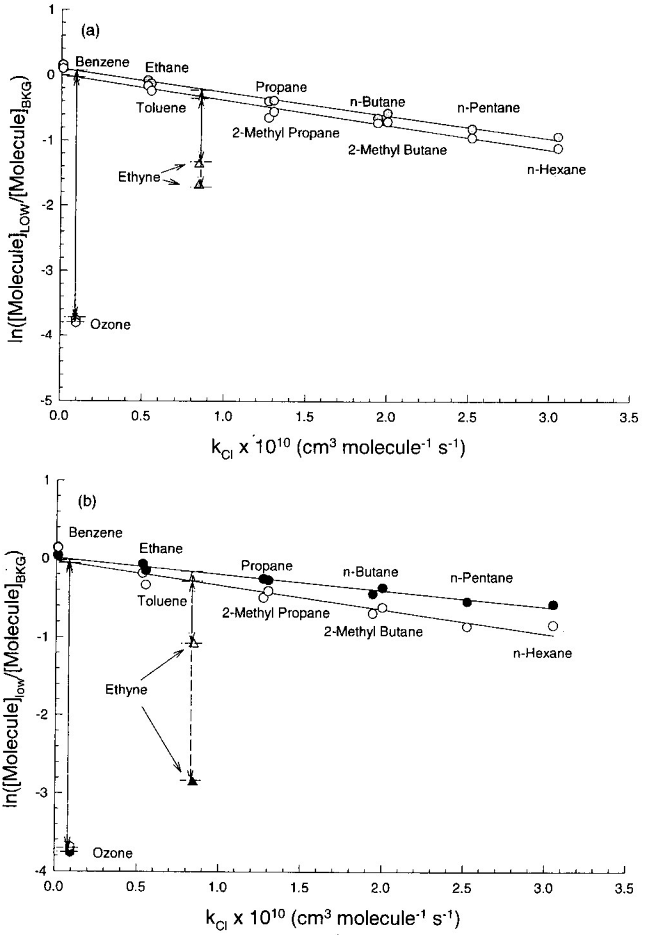

Figure 10. Correlation between logs of hydrocarbon concentration ratios in ozone-depleted air from normal ozone days against Cl atom rate constants for aerial survey on (a) Julian day 89 and (b) Julian day 90, 1994. Least squares fit lines have been drawn through the alkane and benzene data. The deviations of ethyne and ozone from the expected Cl atom kinetics are represented by dashed lines.

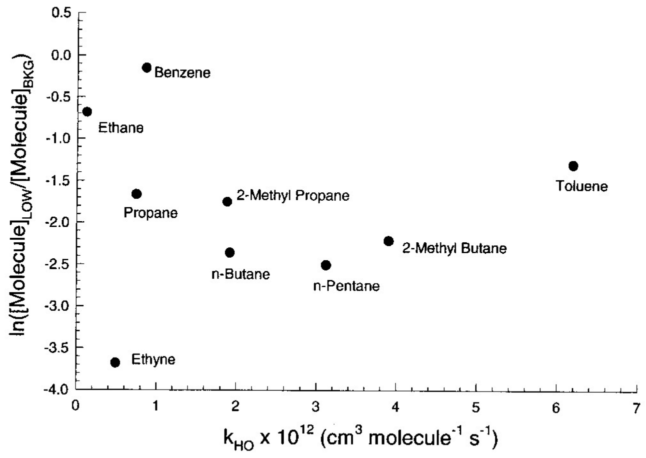

Figure 11. Correlation between the logs of concentration ratios in ozone-depleted air from normal ozone days against HO rate constants for the Julian day 114, 1994, ozone depletion episode at Alert.

ground" values and low-altitude data with ozone depletion as "low" values. The results of this exercise are tabulated in Table 3, in which four pairs of data related to "background" and "low" events were chosen, and Figures 10a and 10b show the kinetic plots according to (4). We did not include higher alkanes due to the high uncertainty in the concentration ratios, since their concentrations during the ozone depletion events were close to or below our quantification limit. Ethene data are also omitted because of the possible contamination effect referred to earlier. To illustrate the selectivity of these kinds of kinetic plots, the hydrocarbon concentration changes for the Julian day 114 episode at Alert are plotted against HO rate constants at 243 K in Figure 11. This plot gives a much poorer fit to the data, and it is clear that the concentration changes are not related to the values of the HO rate constants.

6.6. Ratio of Cl and Br Time Action Integrals

The deviation of ethyne from the least squares fit to the C_2–C_6 alkanes, toluene, and benzene may be a result of additional removal by Br atoms (see Figures 8–10). The occurrence of Br chemistry has previously been suggested to explain the observed decreases in ethyne and ethene observed at Alert [*Bottenheim et al.*, 1990; *McConnell et al.*, 1992; *Jobson et al.*, 1994]. We applied (6) to the ethyne data to estimate the Br atom action integral ($\int$ [Br] dt). The equation describes the observed decrease in ethyne concentration as a result of both Cl and Br atom reactions:

$$\int -k_{\mathrm{Br}}[\mathrm{Br}]\,dt = \ln\left([\mathrm{C_2H_2}]_{\mathrm{low}}/[\mathrm{C_2H_2}]_{\mathrm{bkg}}\right)_{\mathrm{observed}} - \ln\left([\mathrm{C_2H_2}]_{\mathrm{low}}/\mathrm{C_2H_2}]_{\mathrm{bkg}}\right)_{\mathrm{Cl\ atom}} \qquad (6)$$

Since the extent of Cl atom chemistry can be derived from the plots of alkanes, toluene, and benzene (e.g., Figures 8–10), equation (6) can be used to calculate $\int$ [Br] dt and the ratios of $\int$ [Br] $dt/\int$[Cl] dt given in Table 4.

It is to be noted that besides chlorine and bromine, iodine has also been suggested by many researchers to play a role in the troposphere and in the destruction of tropospheric ozone [*Chameides and Davis*, 1980; *Jenkin*, 1993; *Solomon et al.*, 1994]. The reactivity of iodine toward alkanes is established to be very low [e.g., *Nangia and Benson*, 1964]. Hence iodine cannot be responsible for the destruction of alkanes observed during the ozone depletion events in the Arctic. There is no kinetic information on iodine reactions with ethyne; however, recently *Ariya et al.* [1997] indicated that the additional decreases in the concentrations of ethyne, as well as in the concentrations of trichloroethene and tetrachloroethene, during PSE 92 followed Br chemistry.

6.7. Modeling of Ozone Depletion Events

The destruction of ozone by halogen radicals is more complex than that of hydrocarbons due to the existence of catalytic cycles. We used Moccalce to investigate the impact of halogens on ozone. It was assumed that Cl and Br atoms were present simultaneously. Average halogen concentrations were estimated by dividing the observed action integrals by a processing time which was varied in the model. For example, from the average of the action integrals observed at Narwhal and Alert, and assuming a processing time of 5 days, an average [Cl] of 2×10^4 cm^{-3} and an average [Br] of 3×10^7 cm^{-3} were obtained. These concentrations could be sustained in the model using a rate of 2×10^4 cm^{-3} s^{-1} for both Cl_2 and Br_2. Using these values, the model was able to reproduce the observed hydrocarbon decreases and the complete ozone destruction within the given processing time.

We also performed sensitivity studies changing Δt to 10 and 15 days, respectively. Since the time action integrals of Cl and Br did not change, the overall hydrocarbon decay (i.e., [hydrocarbon]$_{low}$/[hydrocarbon]$_{bkg}$) was not affected. It was also found that ozone was almost completely destroyed at the end of the processing time in all model runs. This means that ozone destruction also depends linearly on halogen atom concentration, and that different values of Δt are consistent with the observed hydrocarbon decays.

7. Summary

Daily samples were collected at Alert and Narwhal ice camp from Julian days 90 to 117, 1994, and a 2-day aerial survey over the Arctic region on Julian days 89 and 90, 1994. Several ozone depletion events concurrent with decreases in hydrocarbon concentration relative to their background levels were observed at Alert and Narwhal ice camp. Decreases in hydrocarbon concentrations during the ozone depletion events can be explained by Cl and Br chemistry. Evidence was obtained for Cl atom chemistry occurring in the absence of ozone, and a Cl atom concentration during the ozone depletion event at Narwhal ice camp was estimated. This indicates a Cl atom source that existed during that period and in the absence of ozone. The aerial survey suggests that this phenomenon of ozone depletion coinciding with hydrocarbon decreases covers wide areas of the Arctic region. In addition, the ozone depletions seem to occur only in the planetary boundary layer, and no evidence for free tropospheric ozone depletion was obtained. The Br atom reactions seem to play a major role in the destruction of ozone; Cl atoms can play only a minor role. The integral concentrations of Cl and Br atoms evaluated from the kinetic analysis was sufficient to efficiently destroy ozone in the box model. A crop of papers have recently been published indicating small concentrations of Cl atoms in other marine boundary layer environments [e.g., *Singh et al.*, 1996a; *Wingenter et al.*, 1996]. Recent modeling papers have indicated that the low Cl atom concentrations reported or implied do not have a significant overall impact on marine boundary layer chemistry [*Singh et al.*, 1996b]. However, it is important to note that the results from the Arctic have shown that Br atoms could be even 3 orders of magnitude more abundant than Cl atoms. If Cl atom chemistry is indicative of the presence of Br atoms, then the real question for the marine boundary layer is what is the effect of Br on O_3, if it is indeed present in non-Arctic environments.

Table 4. Estimates of the Time-Integrated Br Atom Concentration

Episode	$\int$ [Br] dt, atoms cm^{-3} s	$\int$ [Br] $dt/\int$ [Cl] dt
Narwhal (Julian day 113)	7.5×10^{12}	922
Alert (Julian day 114)	1.6×10^{13}	1702
Flight (pair 1)	5.2×10^{12}	1676
Flight (pair 2)	1.0×10^{13}	2778
Flight (pair 3)	7.5×10^{12}	1974
Flight (pair 4)	1.7×10^{13}	8095

Data are calculated for 243 K.

Acknowledgments. We thank B. Fu and E. Sugarman for helping with sample analysis, V. Young for assisting with organizing the logistics, H. Dryfhout and S. Ogsten for helping in collecting samples, D. Worthy for providing us methane data, L. Barrie, P. Shepson, and J. McConnell for their helpful comments, C. Weldon for reading over the manuscript, and reviewers for their constructive comments. We acknowledge the Natural Science and Engineering Research Council of Canada (NSERC) and British Gas for financial support. Hiromi Niki was British Gas/Consumer Gas/NSERC/AES chair in atmospheric chemistry and Parisa Ariya is an NSERC graduate fellow.

References

Ariya, P. A., Studies of tropospheric halogen chemistry: Laboratory and field measurements, Ph.D. dissertation, York Univ., North York, Ont., Canada, 1996.

Ariya, P. A., V. Catoire, R. Sander, H. Niki, and G. W. Harris, Trichloroethane and tetrachloroethene: Tropospheric probes for Cl and Br-atom reactions during the polar sunrise, *Tellus, Ser. B, 49*, 583–591, 1997.

Ariya, P. A., H. Niki, and G. W. Harris, Rate constants for the Cl-atom reactions of benzene, ethyne and toluene at T = 296 ± 2 K, *Int. J. Chem. Kinet.*, in press, 1998.

Ariya Hooshiyar, P. A., and H. Niki, Rate constants for the Cl-atom reactions of C_2–C_8 alkanes at T = 296 ± 2 K, *Int. J. Chem. Kinet., 27*, 1197–1206, 1995.

Atkinson, R., Kinetics and mechanisms of the gas phase reactions of the hydroxyl radical with organic compounds under atmospheric conditions, *Chem. Rev., 86*, 69–201, 1986.

Atkinson, R., D. L. Baulch, R. A. Cox, R. F. Hampson Jr., J. A. Kerr, and J. Troe, Evaluated kinetic and photochemical data for atmospheric chemistry: Supplement IV, *J. Phys. Chem. Ref. Data, 21*, 1125–1444, 1992.

Barnes, I., K. H. Becker, and R. D. Overath, Oxidation of organic sulfur compounds, in *The Tropospheric Chemistry of Ozone in The Polar Regions*, edited by H. Niki and K. H. Becker, *NATO ASI Ser., Ser. I*, vol. 17, pp. 371–383, Springer-Verlag, New York, 1993.

Barrie, L. A., J. W. Bottenheim, R. C. Schnell, P. J. Crutzen, and R. A. Rasmussen, Ozone destruction and photochemical reactions at polar sunrise in the lower Arctic atmosphere, *Nature, 334*, 138–141, 1988.

Barrie, L. A., R. Staebler, D. Toom, B. Georgi, G. Den Hartog, S. Landsberger, and D. Wu, Arctic aerosol size-segregated chemical observations in relation to ozone depletion during Polar Sunrise Experiment 1992, *J. Geophys. Res., 99*, 25,439–25,451, 1994.

Bottenheim, J. W., L. A. Barrie, E. Atlas, L. E. Heidt, H. Niki, R. A. Rasmussen, and P. B. Shepson, Depletion of lower tropospheric ozone during Arctic spring: The Polar Sunrise Experiment 1988, *J. Geophys. Res., 95*, 18,555–18,568, 1990.

Chameides, W. L., and D. D. Davis, Iodine: Its possible role in tropospheric photochemistry, *J. Geophys. Res.*, *85*, 7383–7398, 1980.
DeMore, W. B., S. P. Sander, D. M. Golden, R. F. Hampson, M. J. Kurylo, C. J. Howard, A. R. Ravishankara, C. E. Kolb, and M. J. Molina, Chemical kinetic and photochemical data for use in stratospheric modeling, *Eval. 11*, Jet Propul. Lab., Pasadena, Calif., 1994.
Doskey, P. V., and J. S. Gaffney, Non-methane hydrocarbons in the Arctic atmosphere at Barrow, Alaska, *Geophys. Res. Lett.*, *19*, 381–384, 1992.
Fan, S-M., and D. J. Jacob, Surface ozone depletion in the Arctic spring sustained by bromine reactions on aerosols, *Nature*, *359*, 522–524, 1992.
Finlayson-Pitts, B. J., Reactions of NO_2 with NaCl and atmospheric implications of NOCl formation, *Nature*, *306*, 676–677, 1983.
Finlayson-Pitts, B. J., B. J. Ezell, and M. J. Pitts Jr., Formation of chemically active chlorine compounds by reactions of atmospheric NaCl particles with gaseous N_2O_5 and $ClONO_2$, *Nature*, *337*, 241–244, 1989.
Galiba, I., J. M. Tedder, and K. A. Watson, Free-radical substitution in aliphatic compounds, V, The halogenation of 1,1,1-trifluoropentane, *J. Chem. Soc. A*, 1321–1324, 1964.
Hausmann, H., and U. Platt, Spectroscopic measurement of bromine oxide and ozone in the high Arctic during Polar Sunrise Experiment 1992, *J. Geophys. Res.*, *99*, 25,399–25,413, 1994.
Hoigne, J., H. Bader, W. R. Haag, and J. Staehlin, Rate constants of reactions of ozone with organic compounds in water, *Water Res.*, *19*, 993–1004, 1985.
Hopper, J. F., and W. Hart, Meteorological overview of the 1992 Polar Sunrise Experiment, *J. Geophys. Res.*, *99*, 25,315–25,328, 1994.
Hopper, J. F., B. Peters, Y. Yokouchi, H. Niki, B. T. Jobson, P. B. Shepson, and K. Muthuramu, Chemical and meteorological observations at ice camp SWAN during the 1992 Polar Sunrise Experiment, *J. Geophys. Res.*, *99*, 25,489–25,498, 1994.
Hopper, J. F., L. A. Barrie, A. Sills, W. Hart, A. J. Gallant, and H. Dryfhout, Ozone and meteorology during the 1994 Polar Sunrise Experiment, *J. Geophys. Res.*, *103*, 1481–1492, 1998.
Hov, O., S. A. Penkett, I. S. A. Isaksen, and A. Semb, Organic gases in the Norwegian Arctic, *Geophys. Res. Lett.*, *11*, 425–428, 1984.
Jenkin, M. E., A comparative assessment of the role of iodine photochemistry in tropospheric ozone depletion, in *The Tropospheric Chemistry of Ozone in the Polar Regions*, edited by H. Niki and K. H. Becker, *NATO ASI Ser., Ser. I*, vol. 17, pp. 405–416, Springer-Verlag, New York, 1993.
Jobson, B. T., Seasonal trends of nonmethane hydrocarbons at remote boreal and high Arctic sites in Canada, Ph.D. dissertation, York Univ., North York, Ont., Canada, 1994.
Jobson, B. T., H. Niki, Y. Yokouchi, J. Bottenheim, F. Hopper, and R. Leaitch, Measurements of C_2–C_6 hydrocarbons during the Polar Sunrise 1992 Experiment: Evidence for Cl atom and Br atom chemistry, *J. Geophys. Res.*, *99*, 25,355–25,368, 1994.
Keene, W. C., A. A. P. Pszenny, D. J. Jacob, R. A. Duce, J. N. Galloway, J. J. Schultz-Tokos, H. Sievering, and J. F. Boatman, The geochemical cycle of reactive chlorine through the marine troposphere, *Global Biogeochem. Cycles*, *4*, 407–430, 1990.
Kieser, B. N., T. Sideris, H. Niki, J. W. Bottenheim, and W. R. Leaitch, Spring 1989 observations of tropospheric chemistry in the high Arctic, *Atmos. Environ.*, *27*, 2979–2988, 1993.
McConnell, J. C., and G. S. Henderson, Ozone depletion during polar sunrise, in *The Tropospheric Chemistry of Ozone in Polar Regions*, edited by H. Niki and K. H. Becker, *NATO ASI Ser., Ser. I*, vol. 17, Springer-Verlag, New York, 1993.
McConnell, J. C., G. S. Henderson, L. Barrie, J. Bottenheim, H. Niki, C. H. Langford, and E. M. J. Templeton, Photochemical bromine production implicated in Arctic boundary-layer ozone depletion, *Nature*, *355*, 150–152, 1992.
Mickle, R. E., J. W. Bottenheim, W. R. Leaitch, and W. Evans, Boundary layer ozone depletion during AGASP-II, *Atmos. Environ.*, *23*, 2443–2449, 1989.
Mozurkewich, M., Mechanisms for the release of halogens from sea-salt particles by free radical reactions, *J. Geophys. Res.*, *100*, 14,199–14,207, 1995.
Muthuramu, K., P. B. Shepson, J. W. Bottenheim, B. T. Jobson, H. Niki, and K. G. Anlauf, Relationships between organic nitrates and surface ozone destruction during Polar Sunrise Experiment 1992, *J. Geophys. Res.*, *99*, 25,369–25,378, 1994.
Nangia, P. S., and S. W. Benson, The kinetics of dehydrogenation of propane by iodine vapor and the heat of formation of the isopropyl radical, *J. Am. Chem. Soc.*, *86*, 2773–2777, 1964.
Nicovich, J. M., and P. H. Wine, Kinetics of the reaction of O (^{3}P) and Cl (^{2}P) with HBr and Br_2, *Int. J. Chem. Kinet.*, *22*, 379–397, 1990.
Nicovich, J. M., K. D. Kreutter, and P. Wine, Kinetics of the reactions of Cl and Br with ozone, *Int. J. Chem. Kinet.*, *22*, 399–414, 1990.
Oltmans, S. J., L. A. Barrie, E. A. Atlas, L. E. Heidt, H. Niki, R. A. Rasmussen, and P. B. Shepson, Seasonal surface ozone and filterable bromine relationships in the high Arctic, *Atmos. Environ.*, *23*, 2431–2441, 1989.
Pszenny, A. A. P., W. C. Keene, D. J. Jacob, S. Fan, J. R. Maben, M. P. Zewto, M. Springer-Young, and J. N. Galloway, Evidence of inorganic chlorine gases other than hydrogen chloride in maine surface air, *Geophys. Res. Lett.*, *20*, 699–702, 1993.
Russell, J. J., J. A. Seetula, and D. Gutman, Kinetics and thermochemistry of CH_3, C_2H_5, i-C_3H_7: Study of the equilibrium R + HBr $\leftrightarrow$ RH + Br, *J. Am. Chem. Soc.*, *110*, 3092–3099, 1988a.
Russell, J. J., J. A. Seetula, R. S. Timonen, D. Gutman, and D. F. Nava, Kinetics and thermochemistry of the t-C_4H_9 radical: Study of the equilibrium t-C_4H_9 + HBr $\leftrightarrow$ t-C_4H_9 + Br, *J. Am. Chem. Soc.*, *110*, 3084–3991, 1988b.
Sander, R., and P. J. Crutzen, Model study indicating halogen activation and ozone destruction in polluted air masses transported to the sea, *J. Geophys. Res.*, *101*, 9121–9138, 1996.
Sander, R., R. Vogt, G. W. Harris, and P. J. Crutzen, Modeling the chemistry of ozone, halogen compounds and hydrocarbons during Arctic spring, *Tellus, Ser. B*, *49*, 522–532, 1997.
Schroeder, W. H., and P. Urone, Formation of nitrosyl chloride from sea particles in air, *Environ. Sci. Technol.*, *8*, 756–758, 1974.
Singh, H. B., et al., Low ozone in the marine boundary layer of the tropical Pacific Ocean: Photochemical loss, chlorine atoms, and entrainment, *J. Geophys. Res.*, *101*, 1907–1917, 1996a.
Singh, H. B., A. N. Thakur, and Y. E. Chen, Tetrachloroethylene as an indicator of low Cl atom concentrations in the troposphere, *Geophys. Res. Lett.*, *23*, 1529–1532, 1996b.
Solberg, S., O. Hermansen, E. Joranger, N. Schmidtbauer, F. Strodel, and O. Hov, Tropospheric ozone depletion in the Arctic during spring: Measurements on the Zeppelin Mountain on Spitsbergen, *NILU Rep. OR 27/94*, Norw. Inst. for Air Res., Oslo, 1994.
Solberg, S., N. Scmidbauer, A. Semb, F. Strodal, and O. Hov, Boundary layer ozone depletion as seen in the Norwegian Arctic in spring, *J. Atmos. Chem.*, *23*, 301–332, 1996.
Solomon, S., R. R. Garcia, and A. R. Ravishankara, On the role of iodine in ozone depletion, *J. Geophys. Res.*, *99*, 20,491–20,499, 1994.
Staehlin, J., and J. Hoigne, Decomposition of ozone in water: Rate of initiation by hydroxide ions and hydrogen peroxide, *Environ. Sci. Technol.*, *16*, 676–681, 1982.
Warneck, P., *Chemistry of the Natural Atmosphere*, *Int. Geophys. Ser.*, vol. 41, Academic, San Diego, Calif., 1988.
Wingenter, O. W., M. K. Kubo, N. J. Blake, T. W. Smith Jr., D. R. Blake, and F. S. Rowland, Hydrocarbon and halocarbon measurements as photochemical and dynamical indicators of atmospheric hydroxyl, atomic chlorine, and vertical mixing obtained during Lagrangian flights, *J. Geophys. Res.*, *101*, 4331–4340, 1996.
Worthy, D. E. J., N. B. A. Trivett, J. F. Hopper, and J. W. Bottenheim, Analysis of long-range transport events at Alert, Northwest Territories, during the Polar Sunrise Experiment, *J. Geophys. Res.*, *99*, 25,329–25,344, 1994.
Zetzsch, C., and W. Behnke, Heterogeneous reactions of chlorine compounds, in *The Tropospheric Chemistry of Ozone in Polar Regions*, edited by H. Niki and K. H. Becker, *NATO ASI Ser., Ser. I*, vol. 17, pp. 291–306, Springer-Verlag, New York, 1993.

K. J. Anlauf and J. F. Hopper, Atmospheric Environment Service, 4905 Dufferin Street, Downsview, Ontario, Canada M3H 5T4.

P. A. Ariya, Max Planck Institute for Chemistry, Air Chemistry Division, P. O. Box 3060, 55020 Mainz, Germany. (e-mail: parisa@mpch-mainz.mpg.de)

G. W. Harris and R. Sander, Centre for Atmospheric Chemistry and Department of Chemistry, York University, 4700 Keefe Street, North York, Ontario, Canada M3J 1P3.

B. T. Jobson, NOAA Aeronomy Laboratory, 325 Broadway, Boulder, CO 80303.

(Received November 8, 1996; revised January 20, 1998; accepted January 21, 1998.)